

## Optical Rogue Waves in Integrable Turbulence

Pierre Walczak, Stéphane Randoux, and Pierre Suret\*

*Laboratoire de Physique des Lasers, Atomes et Molecules, UMR-CNRS 8523, Université de Lille, France*

(Received 24 October 2014; published 9 April 2015)

We report optical experiments allowing us to investigate integrable turbulence in the focusing regime of the one-dimensional nonlinear Schrödinger equation (1D NLSE). In analogy with broad spectrum excitation of a one-dimensional water tank, we launch random initial waves in a single mode optical fiber. Using an original optical sampling setup, we measure precisely the probability density function of optical power of the partially coherent waves rapidly fluctuating with time. The probability density function is found to evolve from the normal law to a strong heavy-tailed distribution, thus revealing the formation of rogue waves in integrable turbulence. Numerical simulations of 1D NLSE with stochastic initial conditions quantitatively reproduce the experiments. Our numerical investigations suggest that the statistical features experimentally observed rely on the stochastic generation of coherent analytic solutions of 1D NLSE.

DOI: [10.1103/PhysRevLett.114.143903](https://doi.org/10.1103/PhysRevLett.114.143903)

PACS numbers: 42.65.Sf, 05.45.-a

The field of nonlinear optics has recently grown as a favorable laboratory to investigate both statistical properties of nonlinear random waves and hydrodynamiclike phenomena [1–3]. In particular, several recent works point out analogies between hydrodynamics and nonlinear fiber optics in the observation of supercontinuum generation [4], undular bores [2], optical turbulence, laminar-turbulent transition [1], or oceanographic rogue waves (RW) [5,6].

Rogue waves, also called freak waves, are extremely large amplitude waves occurring more frequently than expected from the normal law [7,8]. Since the pioneering work of Solli *et al.* in 2007 [5], optical RW have been studied in various contexts, such as supercontinuum generation in fibers [5,9–11], laser filamentation, [12] passive cavities [13], lasers [14–16], and Raman fiber amplifiers [17].

As stressed in the recent review [6], there is no obvious analogy between most of the optical experiments on extreme events and oceanography. However, a direct correspondence between nonlinear optics and hydrodynamics is provided by the one-dimensional nonlinear Schrödinger equation (1D NLSE) [see Eq. (1)] that describes various wave systems [6,18]. In particular, the focusing 1D NLSE describes at leading order the physics of deep-water wave trains and it plays a central role in the study of RW [6–8,18,19].

Modulational instability (MI) is believed to be a fundamental mechanism for the formation of RW [8,20]. Moreover, analytical solutions of the integrable 1D NLSE, such as Akhmediev breathers (AB), Peregrine solitons or Kuznetsov-Ma solitons (KMs), are now considered as possible prototypes of RW [19,21–23]. These coherent structures have been generated from very specific, carefully designed coherent initial conditions in optical fiber experiments [21,23,24].

On the contrary, oceanic RW emerge from the interplay of incoherent waves in turbulent systems. The appropriate theoretical framework combining a statistical approach of

random waves together with the 1D NLSE is integrable turbulence. This emerging fundamental field of research recently introduced by Zakharov relies on the analysis of complex phenomena found in nonlinear random waves systems described by an integrable equation [25–30]. The mechanisms found in integrable turbulence are of a profoundly different nature than those found in conventional turbulence [3,25,30].

The initial conditions under consideration in the recent theoretical studies of integrable turbulence are formed by a condensate with additional noise [28]. Surprisingly, in this case, MI does not lead to higher occurrence of extreme events than predicted by the central limit theorem. On the contrary, using incoherent initial conditions, deviation from Gaussian statistics has been predicted in the weakly nonlinear regime [31]. In hydrodynamical experiments made with one-dimensional water tanks, non-Gaussian statistics of the wave height have also been found to emerge from random initial conditions [20,32].

Nonlinear fiber optics is a promising field for the investigation of integrable turbulence because optical tabletop “model experiments” precisely described by the 1D NLSE can be performed [21,23,24,29]. For instance, the statistical properties of slowly fluctuating random waves in defocusing integrable turbulence have been studied recently [29]. As MI easily broadens the optical spectrum beyond the bandwidth of standard photodetectors, the experimental study of the focusing integrable turbulence is very challenging. Despite the numerous works devoted to optical RW, the generation of extreme events from purely stochastic initial conditions in focusing 1D NLSE model experiments remains a crucial and open question [6,19,28,33].

In this Letter, we address the fundamental problem of the propagation of random waves described by the focusing 1D NLSE [26,28,33–35]. We implement an optical fiber

experiment conceptually analogous to the water tank experiment described in Ref. [20]. Using an original setup to overcome bandwidth limitations of usual detectors, we evidence strong distortions of the statistics of nonlinear random light characterizing the occurrence of optical rogue waves in integrable turbulence.

The response times of conventional detectors are usually slower than the typical time scale characterizing power fluctuations of incoherent optical waves (see Supplemental Material, Sec. II [36]). Since the work of Solli *et al.*, spectral filters are therefore often used to reveal extreme events in time-domain experiments [5,10,16]. In addition to these filtering techniques, shot-to-shot spectrum fluctuations can be evidenced with a dispersive Fourier transform measurement in experiments of pulsed supercontinuum generation [5,37–39]. Performing an accurate and well-calibrated measurement of the probability density function (PDF) characterizing temporal power fluctuations of *random light* is still a challenging task in the field of nonlinear statistical optics.

We have developed an original setup that allows the precise measurement of statistics of random light rapidly fluctuating with time. Inspired by the time-resolved fluorescence up-conversion experiments [40] and by the optical sampling oscilloscope [41], the principle of our method is based on asynchronous optical sampling [see Fig. 1(a)].

Our experimental setup is schematically shown in Fig. 1(b). A “continuous wave” ytterbium fiber laser (IPG-YLR series) emitting a linearly polarized partially coherent wave at  $\lambda_S = 1064$  nm is used as a random light source. This cw laser emits numerous (typically  $10^4$ ) uncorrelated longitudinal modes. The partially coherent wave under investigation is called the signal. Blue pulses are generated at a wavelength  $\lambda = 457$  nm by sum-frequency generation (SFG) between the signal at  $\lambda_S = 1064$  nm and short pump pulses having a central wavelength  $\lambda_p = 800$  nm. SFG is achieved in a  $5 \times 5 \times 8$  mm BBO crystal. Noncollinear type I phase matching is achieved with an external angle of  $10^\circ$  between the pump and the signal [42,43].

The 140-fs-long pump pulses are emitted by a mode-locked Ti:sapphire laser (Coherent Cameleon ultra II) with a repetition rate of 80 MHz. The maximum output power of the fiber laser is much weaker than the peak power ( $\approx 4 \cdot 10^5$  W) of the pump pulses. The pump pulses remain, therefore, undepleted and the peak powers of SFG pulses are proportional to the instantaneous optical powers  $P = P_{(\lambda_S=1064 \text{ nm})}$  carried by the signal [42]. The SFG pulses’ power [solid red line in Fig. 2(a)] can be seen as periodic snapshots of the fluctuating optical power  $P$  carried by the signal. We compute the PDF of  $P$  from the statistical distribution of the peak powers of the SFG pulses [red line in Fig. 2(b)].

The short blue pulses are observed by using a highly sensitive photodiode (MenloSystem FPD310-FV) having a gain of  $\approx 10^4$  and a rise time of 0.7 ns. We record the output

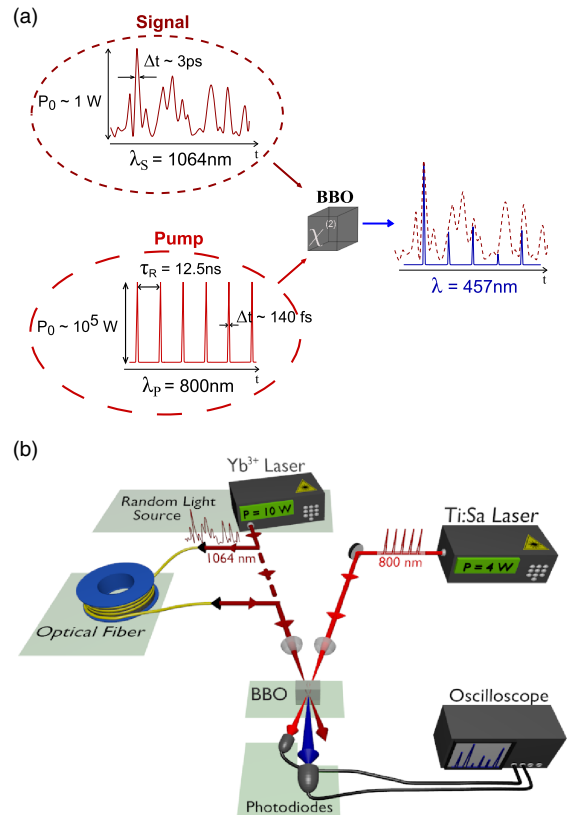


FIG. 1 (color online). Measurement of the statistics of random light. (a) Principle. Optical sampling of the partially coherent wave fluctuating with time (the signal) is achieved from SFG. Blue pulses are generated at  $\lambda = 457$  nm from the interaction of the signal with femtosecond pump pulses inside a  $\chi^{(2)}$  crystal. (b) Setup. The 140 fs pump pulses are emitted by mode-locked laser at  $\lambda_p = 800$  nm. The partially coherent wave is emitted by a ytterbium fiber laser at  $\lambda_S = 1064$  nm. Statistics of partially coherent light is measured from the SFG process either directly at the output of the laser or after propagation inside an optical fiber.

of the photodiode with a fast oscilloscope (Lecroy WaveRunner 104MXi-A, bandwidth 1 GHz, 10 GS/s). We have carefully used the photodiode in a linear regime without any saturation effect. The peak voltage is proportional to the energy of the corresponding optical pulse. A second photodiode is used to record pump pulses with a high signal-to-noise ratio. This provides a synchronization signal permitting us to identify the maxima of SFG pulses. The normalized PDF of the signal is computed from an ensemble of approximately  $16 \times 10^6$  measurements of SFG peak powers.

We first measure the PDF at the output of the laser. In all experiments presented in this Letter, the mean output power of the ytterbium laser is fixed at  $\langle P \rangle = 10$  W. At this operating point, the statistics of the partially coherent wave follows the normal law. Indeed, as plotted in Fig. 2(b), the PDF of the normalized power  $P/\langle P \rangle$  is very close to the exponential function [see Fig. 2(b)]. Assuming that the real

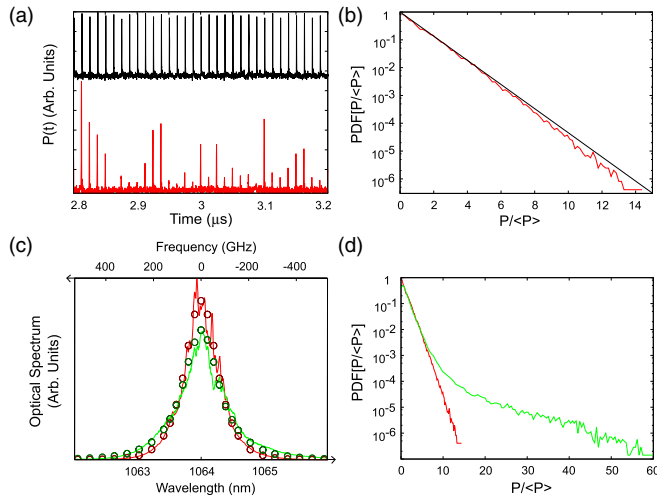


FIG. 2 (color online). Experiments. (a) Pump pulses (black line) and samples of fiber laser fluctuations (SFG pulses, red line). (b) Statistics of fluctuations at the output of the fiber laser. Probability density function (PDF) of normalized optical power  $P/\langle P \rangle$  (red line). The PDF is computed from SFG peak powers plotted in (a). Normalized exponential distribution  $\text{PDF}[P/\langle P \rangle] = \exp(-P/\langle P \rangle)$  (black line) (c),(d) Focusing propagation. Optical power spectra (c) and PDFs (d) of the partially coherent wave at the input (red line) and output (green line) of the fiber. Experiments are plotted with solid lines [(c),(d)] and numerical simulations are plotted with circles (c).

part and the imaginary parts are statistically independent, this exponential distribution of power corresponds to a Gaussian statistics of the field. It is important to note that the black line in Fig. 2(b) is not a fitted exponential function, but it represents the exact normalized  $\text{PDF}[P/\langle P \rangle] = \exp(-P/\langle P \rangle)$ . To the best of our knowledge, the PDF of so rapidly fluctuating optical signals has never been quantitatively compared to the normalized exponential distribution.

We now use the output of the laser as a random source and we launch the partially coherent signal into an optical fiber in the focusing regime. The fiber is a 15-m-long highly nonlinear photonic crystal fiber (provided by Draka France Company) having an anomalous dispersion at 1064 nm. The fiber maintains the polarization of light, and single transverse mode propagation is also achieved. A random light wave with a mean power  $\langle P \rangle = 600$  mW is launched into the fiber.

Experiments have been carefully designed to be very well described by the 1D NLSE. In particular, the signal wavelength  $\lambda_s = 1064$  nm is far from the zero-dispersion wavelength  $\lambda_0 \approx 970$  nm. Moreover, the optical spectral widths [see Fig. 2(c)] remain sufficiently narrow to neglect stimulated Raman scattering and high-order dispersion effects (see Supplemental Material [36]). The linear losses experienced by optical fields in single pass in the fibers are very negligible. These total losses are around 0.3% in the fiber (loss coefficient of 8 dB/km).

The measurement of the statistics of the optical power after propagation of the partially coherent field in the fiber reveals the occurrence of numerous extreme events (RW). The comparison between the initial PDF [see red line in Fig. 2(d)] and the output PDF [see green curve in Fig. 2(d)] shows an impressive change in the statistical distribution of optical power. The initial field follows the normal law and its PDF is an exponential function, whereas the output PDF of optical power exhibits a strong heavy tail. The probability of occurrence of very high powers fluctuations (more than 10 times greater than the mean power) is much larger than the probability defined by the normal law. As an example, a fluctuation with a power greater than 50 times the mean power almost never occurs in the initial random Gaussian field (one intense fluctuation every  $10^{10}$  s), whereas it occurs every  $10^{-6}$  s at the output of the fiber.

We have performed numerical simulations of the 1D NLSE

$$i \frac{\partial \psi}{\partial z} = \frac{\beta_2}{2} \frac{\partial^2 \psi}{\partial t^2} - \gamma |\psi|^2 \psi, \quad (1)$$

with parameters corresponding to the experiments. At  $\lambda_s = 1064$  nm, the group velocity dispersion coefficient of the fiber is  $\beta_2 = -20$  ps<sup>2</sup>/km. The effective Kerr coefficient is  $\gamma = 50$  W<sup>-1</sup> km<sup>-1</sup>.

Numerical simulations are performed by discretizing a temporal window of 618 ps with a set of 8192 points and by using a pseudospectral split-step-based method. Mean optical power spectra and PDFs are computed from Monte Carlo simulations performed over an ensemble of 4000 realizations of the initial random process. Assuming stationary statistics, the initial field is computed in the Fourier space for each realization of the random initial condition with the random phase procedure [30,44,45]:  $\tilde{\psi}(\omega) = \sqrt{n(\omega)} \exp(i\phi_\omega)$ , where  $\phi_\omega$  is a white delta-correlated random process. From best-fit procedures applied to the laser optical spectrum experimentally recorded, we take an initial spectrum  $n(\omega) = n_0 \text{sech}(\omega/\Delta\omega)$  with  $\Delta\omega = 2\pi \times 63$  GHz.

Optical spectra [see circles in Fig. 2(c)] and PDFs [see solid green line in Fig. 3(a)] computed from the numerical integration of the 1D NLSE are in quantitative and remarkable agreement with experiments. The comparison between experiments and simulations proves that statistical distributions found in experiments are very well described by the integrable 1D NLSE.

Numerical simulations of 1D NLSE allow us to explore the statistics of the wave system at long propagation distances. This is not feasible in the experiment because other effects, such as stimulated Raman scattering, may play a non-negligible role and break the integrability of the wave system. In the experiment, the nonlinear Kerr length  $L_{\text{NL}} = 1/(\gamma P_0) \approx 30$  m and the linear dispersive length  $L_D = 1/[\beta_2 (2\pi\Delta\nu_0)^2] \approx 10$  m, where  $\Delta\nu_0 = 340$  GHz is the full width at  $1/e^2$  of the spectrum (see Supplemental

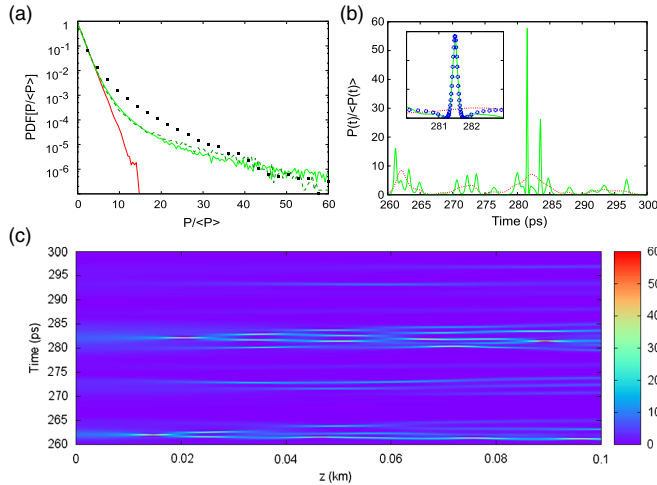


FIG. 3 (color online). Numerical simulations. (a). PDF of optical power at a propagation length  $z = 0$  m (solid red line),  $z = 15$  m (solid green line), and  $z = 100$  m (stationary state, black squares). Experimental PDF ( $z = 15$  m) of Fig. 2(d) is displayed for comparison (dashed green line). (b),(c) Typical temporal optical power fluctuations along the nonlinear propagations. Green line in (c): fluctuations at  $z = 90$  m. Inset in (b): enlarged view of an intense power fluctuation superimposed on the profile of a Peregrine soliton (blue circle) determined from a best-fit procedure.

Material [36] and Ref. [46]). With the parameters corresponding to our experiments, numerical simulations show that the spectrum and the PDF reach a stationary state characterized by a strongly heavy-tailed PDF for a fiber length  $L \approx 100$  m [see black squares in Fig. 3(a)].

In our experiments, the frequency at which the gain of the MI process is maximum (275 GHz) lies within the wings of the spectrum of the initial incoherent wave [see Fig. 2(c)]. On the contrary, the authors of Ref. [28] study numerically the nonlinear stages of the MI of the condensate. In this case the stationary statistics follows the normal law, which means that the probability of RW formation is the same as in a linear wave system. It is not surprising in integrable systems that the nature of the stationary state depends on the initial conditions. However, further theoretical investigations are needed to fully characterize this remarkable difference between two stationary states of integrable turbulence.

Numerical simulations give some insight into the mechanisms underlying the breakdown of the Gaussian statistics observed in our experiments. In the focusing propagation, solitons on finite background such as AB, Peregrine solitons, or KMs having a short duration and a high power seem to emerge on the top of the highest fluctuations [see the example of the Fig. 3(b)]. Note that the emergence of such coherent structures in incoherent fields has already been theoretically studied in nonintegrable wave turbulence [47,48] and in integrable turbulence emerging from a modulationally unstable condensate [26,28,33].

Our experiment made in the anomalous dispersion regime is qualitatively comparable to one-dimensional deep-water-wave experiments. Starting from random initial conditions, hydrodynamical experiments have demonstrated the formation of heavy-tailed statistics [20,32,49]. However, in water-wave experiments, the extreme events are far less frequent because the height of the waves is strongly limited by the phenomenon of wave breaking [50]. In hydrodynamics, relatively small deviations from Gaussianity have been observed and interpreted in the framework of wave turbulence theory [8,31,51]. On the contrary, our optical fiber setup provides an accurate laboratory for the exploration of strongly nonlinear random wave systems ruled by the 1D NLSE.

Note that deviations from Gaussian statistics have been reported in 1D spatial experiments in which the transverse intensity profile of optical beams randomly fluctuating with space is easily recorded by using cameras [8,52]. In spatial experiments, the speckle fields are localized [52,53] and the dynamics of random waves is confined in a way comparable to the one found in experiments with light pulses [54]. Our experiments with nondecaying random waves widen the perspectives of experimental integrable turbulence studies.

The results presented in this Letter do not only provide fundamental results on RW in integrable turbulence, but they also demonstrate a powerful method to study the statistics of optical fields rapidly fluctuating with time. We have estimated from annex experiments that the statistics of temporal fluctuations as short as 250 fs can be accurately measured with our setup (see Supplemental Material, Sec. I [36]). Our method enables, for example, statistical study of fiber lasers (see Supplemental Material, Sec. III [36]), which are remarkable systems for the investigation of optical turbulence [1].

In this Letter, we have quantified how the statistics of stochastic nonlinear optical fields strongly deviate from the normal law in an optical fiber experiment. Our experiments are very well described by the integrable focusing 1D NLSE and they prove that RW can appear in integrable turbulence [26,28,34]. Our numerical results strengthen the idea that the emergence of deterministic solutions of 1D NLSE, such as AB, Peregrine solitons, or KMs in nonlinear random fields, is a major mechanism for the formation of rogue waves [6,19,55]. From our work, we hope to stimulate further theoretical and experimental investigations intending to establish a clear connection between the emergence of coherent structures and the statistical properties of nonlinear stochastic fields.

This work was supported by the Labex CEMPI (ANR-11-LABX-0007-01) and by the French National Research Agency (ANR-12-BS04-0011 OPTIROC). The authors acknowledge S. Bielawski for fruitful discussions. The authors acknowledge R. Habert, C. Szwaj, and E. Roussel for technical help. The authors acknowledge Draka France Company, which has provided the fiber.

- \*Corresponding author.  
Pierre.Suret@univ-lille1.fr
- [1] E. G. Turitsyna, S. V. Smirnov, S. Sugavanam, N. Tarasov, X. Shu, S. B. E. Podivilov, D. Churkin, G. Falkovich, and S. Turitsyn, *Nat. Photonics* **7**, 783 (2013).
- [2] J. Fatome, C. Finot, G. Millot, A. Armaroli, and S. Trillo, *Phys. Rev. X* **4**, 021022 (2014).
- [3] A. Picozzi, J. Garnier, T. Hansson, P. Suret, S. Randoux, G. Millot, and D. Christodoulides, *Phys. Rep.* **542**, 1 (2014).
- [4] A. Chabchoub, N. Hoffmann, M. Onorato, G. Genty, J. M. Dudley, and N. Akhmediev, *Phys. Rev. Lett.* **111**, 054104 (2013).
- [5] D. R. Solli, C. Ropers, P. Koonath, and B. Jalali, *Nature (London)* **450**, 1054 (2007).
- [6] J. M. Dudley, F. Dias, M. Erkintalo, and G. Genty, *Nat. Photonics* **8**, 755 (2014).
- [7] M. Onorato, A. R. Osborne, M. Serio, and S. Bertone, *Phys. Rev. Lett.* **86**, 5831 (2001).
- [8] M. Onorato, S. Residori, U. Bortolozzo, A. Montina, and F. Arecchi, *Phys. Rep.* **528**, 47 (2013).
- [9] D. R. Solli, C. Ropers, and B. Jalali, *Phys. Rev. Lett.* **101**, 233902 (2008).
- [10] M. Erkintalo, G. Genty, and J. M. Dudley, *Opt. Lett.* **34**, 2468 (2009).
- [11] B. Kibler, C. Finot, and J. M. Dudley, *Eur. Phys. J. Spec. Top.* **173**, 289 (2009).
- [12] J. Kasparian, P. B ejot, J.-P. Wolf, and J. M. Dudley, *Opt. Express* **17**, 12070 (2009).
- [13] A. Montina, U. Bortolozzo, S. Residori, and F. T. Arecchi, *Phys. Rev. Lett.* **103**, 173901 (2009).
- [14] C. Bonatto, M. Feyerreisen, S. Barland, M. Giudici, C. Masoller, J. R. Rios Leite, and J. R. Tredicce, *Phys. Rev. Lett.* **107**, 053901 (2011).
- [15] C. Lecaplain, P. Grelu, J. M. Soto-Crespo, and N. Akhmediev, *Phys. Rev. Lett.* **108**, 233901 (2012).
- [16] S. Randoux and P. Suret, *Opt. Lett.* **37**, 500 (2012).
- [17] K. Hammani, C. Finot, J. M. Dudley, and G. Millot, *Opt. Express* **16**, 16467 (2008).
- [18] J. Dudley, C. Finot, G. Millot, J. Garnier, G. Genty, D. Agafontsev, and F. Dias, *Eur. Phys. J. Spec. Top.* **185**, 125 (2010).
- [19] N. Akhmediev, J. M. Dudley, D. R. Solli, and S. K. Turitsyn, *J. Opt.* **15**, 060201 (2013).
- [20] M. Onorato, A. R. Osborne, M. Serio, L. Cavaleri, C. Brandini, and C. T. Stansberg, *Phys. Rev. E* **70**, 067302 (2004).
- [21] B. Kibler, J. Fatome, C. Finot, G. Millot, F. Dias, G. Genty, N. Akhmediev, and J. M. Dudley, *Nat. Phys.* **6**, 790 (2010).
- [22] A. Chabchoub, N. P. Hoffmann, and N. Akhmediev, *Phys. Rev. Lett.* **106**, 204502 (2011).
- [23] B. Kibler, J. Fatome, C. Finot, G. Millot, G. Genty, B. Wetzal, N. Akhmediev, F. Dias, and J. M. Dudley, *Sci. Rep.* **2**, 463 (2012).
- [24] B. Frisquet, B. Kibler, and G. Millot, *Phys. Rev. X* **3**, 041032 (2013).
- [25] V. E. Zakharov, *Stud. Appl. Math.* **122**, 219 (2009).
- [26] V. E. Zakharov and A. A. Gelash, *Phys. Rev. Lett.* **111**, 054101 (2013).
- [27] E. Pelinovsky, E. Shurgalina, A. Sergeeva, T. Talipova, G. El, and R. Grimshaw, *Phys. Lett. A* **377**, 272 (2013).
- [28] D. S. Agafontsev and V. E. Zakharov, arXiv:1409.4692.
- [29] S. Randoux, P. Walczak, M. Onorato, and P. Suret, *Phys. Rev. Lett.* **113**, 113902 (2014).
- [30] P. Suret, A. Picozzi, and S. Randoux, *Opt. Express* **19**, 17852 (2011).
- [31] P. A. E. M. Janssen, *J. Phys. Oceanogr.* **33**, 863 (2003).
- [32] M. Onorato, A. Osborne, M. Serio, and L. Cavaleri, *Phys. Fluids* **17**, 078101 (2005).
- [33] N. Akhmediev, J. Soto-Crespo, and A. Ankiewicz, *Phys. Lett. A* **373**, 2137 (2009).
- [34] D. Agafontsev, *JETP Lett.* **98**, 731 (2014).
- [35] S. K. Turitsyn and S. A. Derevyanko, *Phys. Rev. A* **78**, 063819 (2008).
- [36] See Supplemental Material at <http://link.aps.org/supplemental/10.1103/PhysRevLett.114.143903> for data and discussions about the temporal resolution of PDF measurements, about the ytterbium laser statistics and about side-effects such as stimulated Raman scattering.
- [37] B. Jalali, D. Solli, K. Goda, K. Tsia, and C. Ropers, *Eur. Phys. J. Spec. Top.* **185**, 145 (2010).
- [38] B. Wetzal *et al.*, *Sci. Rep.* **2**, 882 (2012).
- [39] K. Goda and B. Jalali, *Nat. Photonics* **7**, 102 (2013).
- [40] H. Mahr and M. D. Hirsch, *Opt. Commun.* **13**, 96 (1975).
- [41] M. A. Duguay and J. W. Hansen, *Appl. Phys. Lett.* **13**, 178 (1968).
- [42] R. W. Boyd, *Nonlinear Optics* (Academic Press, San Diego, 1992).
- [43] H. Rhee and T. Joo, *Opt. Lett.* **30**, 96 (2005).
- [44] S. Nazarenko, *Wave Turbulence*, Lecture Notes in Physics Vol. 825 (Springer-Verlag, Berlin, 2011), ISBN .
- [45] B. Barvau, S. Randoux, and P. Suret, *Opt. Lett.* **31**, 1696 (2006).
- [46] G. P. Agrawal, *Nonlinear Fiber Optics*, 3rd ed., Optics and Photonics (Academic Press, New York, 2001).
- [47] K. Hammani, B. Kibler, C. Finot, and A. Picozzi, *Phys. Lett. A* **374**, 3585 (2010).
- [48] B. Kibler, K. Hammani, C. Michel, C. Finot, and A. Picozzi, *Phys. Lett. A* **375**, 3149 (2011).
- [49] H. D. Zhang, C. Guedes Soares, Z. Cherneva, and M. Onorato, *Nat. Hazards Earth Syst. Sci.* **14**, 959 (2014).
- [50] A. Iafra, A. Babanin, and M. Onorato, *Phys. Rev. Lett.* **110**, 184504 (2013).
- [51] N. Mori, M. Onorato, and P. A. E. M. Janssen, *J. Phys. Oceanogr.* **41**, 1484 (2011).
- [52] Y. Bromberg, U. Lahini, E. Small, and Y. Silberberg, *Nat. Photonics* **4**, 721 (2010).
- [53] S. Derevyanko and E. Small, *Phys. Rev. A* **85**, 053816 (2012).
- [54] D. Solli, G. Herink, B. Jalali, and C. Ropers, *Nat. Photonics* **6**, 463 (2012).
- [55] J. M. Dudley, G. Genty, F. Dias, B. Kibler, and N. Akhmediev, *Opt. Express* **17**, 21497 (2009).